AD-A062 353 VIRGINIA POLYTECHNIC INST AND STATE UNIV BLACKSBURG --ETC F/G 20/4
NORMAL SHOCK INTERACTION WITH A TURBULENT BOUNDARY LAYER ON A C--ETC(U)
OCT 78 G R INGER, H SOBIECZKY N00014-75-C-0456

UNCLASSIFIED VPI-AERO-088 NL

1 OF 1
AD
A062353

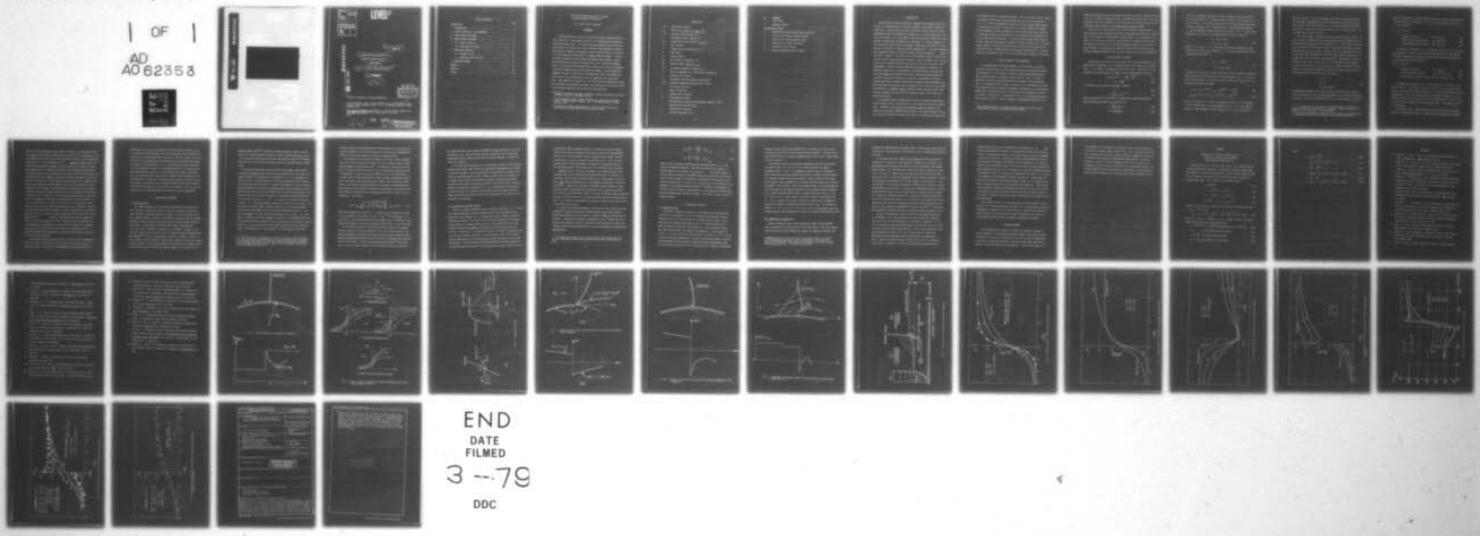

END
DATE
FILMED
3 -79
DDC

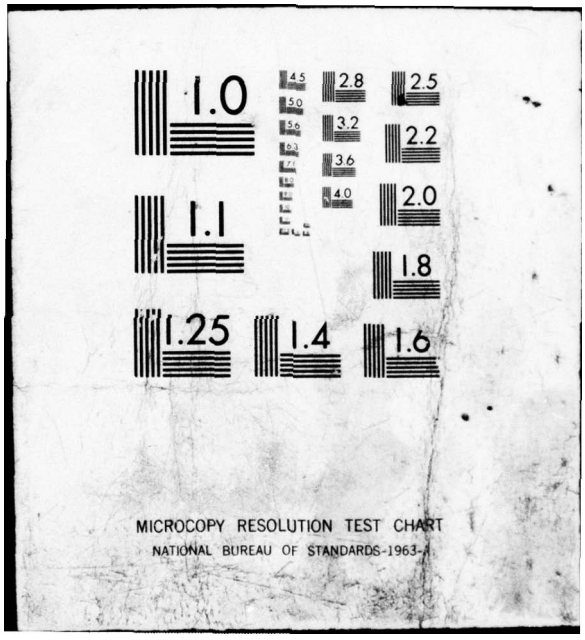
1.0
1.1
1.25
1.4
1.6
1.8
2.0
2.2
2.5
2.8
3.2
3.6
4.0
4.5
5.0
5.6
MICROCOPY RESOLUTION TEST CHART
NATIONAL BUREAU OF STANDARDS-1963-A

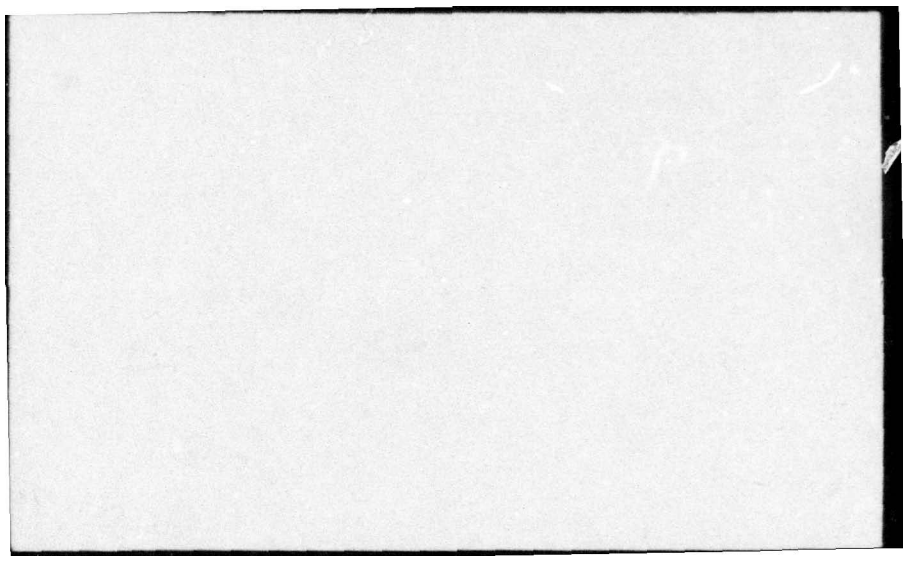

LEVEL II

(14) VPI-Aero-088

(6) NORMAL SHOCK INTERACTION with a TURBULENT BOUNDARY LAYER on a CURVED WALL*

(10) G. R. Inger† and H. Sobieczky††

(11) Oct[redacted]78

(12) 44p.

† Professor of Aerospace and Ocean Engineering.

†† Visiting Professor, Dept. of Aero and Mech. Eng., University of Arizona, Tucson, Arizona; permanent address, Inst. für Strömungs-mechanik, DFVLR, Göttingen, FRG.

* Based on joint research supported by U. S. Office of Naval Research Contract (15) N00014-75-C-0456 (GRI) and NASA Contract 2112 (HS).

Table of Contents

Normal Shock Interaction With a Turbulent Boundary Layer on a Curved Wall*

G. R. Inger† and H. Sobieczky††

Abstract

A detailed analysis is made of longitudinal surface curvature effects on the interaction of a weak normal shock with a non-separating two-dimensional turbulent boundary layer. It is shown that the interactive viscous displacement effect on the local outer inviscid transonic flow completely eliminates the well-known singularity pertaining to purely inviscid flow on a curved wall, i.e., the interactive pressure field is regular behind the shock. A study of the inner interaction solution within the boundary layer, however, reveals that curvature can influence the interaction but for a hitherto-overlooked reason: the effect on the turbulent eddy viscosity, which alters the boundary layer profile shape upon which the interaction depends. An approximate non-asymptotic solution is given which incorporates this effect and example numerical results are presented and verified by comparison with experimental data. Small amounts of curvature ($K \cdot \delta \sim .01$-$.02$) are found to moderately spread out and thicken the interaction zone while also beneficially delaying the onset of any incipient separation that occurs under the shock foot.

---

† Professor of Aerospace and Ocean Engineering, Virginia Polytechnic Institute and State University, Blacksburg, VA, USA.

†† Visiting Professor, Dept. of Aero and Mech. Eng., University of Arizona, Tucson, Arizona; permanent address, Inst. für Strömungs mechanik, DFVLR, Göttingen, FRG.

* Based on joint research supported by U.S. Office of Naval Research Contract N00014-75-C-0456 (GRI) and NASA Contract 2112 (HS).

Nomenclature

a^*	Sonic speed of sound
C_f	Skin friction coeff. $(= 2\tau_w/\rho_{e_1} U_{e_1}^2)$
F,G	Functions defined in Eqs. 4, 7
h	Body shape function, see Fig. 4
H_i	Incompressible form factor $(= \delta_i^*/\theta_i^*)$
K	Wall curvature
L	Distance to shock location (Fig. 7)
M	Mach number
p	Static pressure
R_B	Wall radius of curvature $(\simeq K^{-1})$
Re_L	Reynolds number $(= \rho_{e_1} U_{e_1} L/\mu_{e_1})$
s,t	Transformed dependent variables, Eq. 1
u,v	Velocity components in x,y directions, respectively
w	Resultant flow velocity
x,y	Coordinates along and normal to body surface
X,Y,Z	Stretched independent variables, Eqs. 2 and 5
β	Shock wave angle, Fig. 3
γ	Specific heat ratio
δ	Boundary layer thickness
δ^*	Displacement thickness
η	Non-dimensional interactive displacement thickness, Fig. 7
ν	Resultant flow direction angle
μ	Coefficient of viscosity
σ	Similarity parameter, Eq. 2

ρ	Density
τ	Shear stress
θ^*	Momentum thickness

Sub and Super-scripts

0	Undisturbed incoming boundary layer properties
1	Inviscid flow conditions ahead of shock
2	Inviscid flow conditions behind shock
e	Conditions at boundary layer edge
w	Conditions at wall surface
( )'	denotes perturbation from "0" state

1. INTRODUCTION

The influence of surface curvature on transonic shock-boundary layer interaction is an important basic and practical question, since these interactions often occur on curved surfaces and have significant effects on the flow around aerodynamic bodies and cascade/turbine blades and on internal flows within channels and diffusors. As is well-known, Oswatitsch and Zierep[1] studied the related problem of normal shock impingement on a curved wall in a purely inviscid flow; they found that convex curvature introduces a logarithmic singularity in the wall pressure in the form of a sharp post-shock expansion (Fig. 1) and this phenomenon has indeed been observed in inviscid numerical solutions by Emmons[2], Jameson[3] and others. However, in real flows even at high Reynolds numbers, viscous smearing and upstream influence effects arise due to the thin boundary layer along the surface which profoundly influence the physics of the local interactive flow[4,5]. Consequently, in view of the well-known role often played by viscosity in eliminating singularities, one would expect the boundary layer to significantly alter and perhaps even eliminate this inviscid curvature-induced singularity. Yet such a singularity continues to be cited as an explanation of various features observed in transonic shock-turbulent boundary layer experiments along curved walls and also has been used (erroneously in our view) as an outer boundary condition in a proposed viscous interaction theory for curved walls[6]; thus a proper treatment of the role of wall curvature in real viscous flows still remains to be given.

In the present paper, we address this issue for the case of a weak nearly-normal transonic shock interacting with a 2-D non-separating turbulent boundary layer. Following a brief overview of the general physical features of the problem, we first make a detailed analysis of the local mixed transonic inviscid flow structure outside the boundary layer when it is interactively coupled with

the attendant thickness response of the layer. The results show that the viscous displacement effect eliminates the aforementioned wall-curvature singularity, i.e., it is in fact a mathematical creature of a purely inviscid model and the true influence of curvature of the outer flow is actually quite well-behaved. We then examine the inner disturbance flow within the boundary layer, where it is shown that surface curvature does exert an influence on the interaction, but from a hitherto-overlooked source: its effect on the turbulent eddy viscosity. Using an approximate non-asymptotic method of solution to account for this effect, example numerical results are given for typical interaction and shown to be in accord with Ackeret, Feldman and Rott's experimental observations[4]. A re-interpretation of curved wall data in the light of the present findings is also given.

2. TYPICAL FEATURES OF THE INTERACTION

As a background for the present approach, we first briefly outline the principal physical features of a non-separating normal shock-turbulent boundary layer interaction. To fix ideas, we consider an undisturbed equilibrium turbulent boundary layer in the Reynolds number range $10^5 \lesssim Re_L \lesssim 10^8$ that is perturbed by a normal or nearly-normal shock weak enough to avoid separation ($M_1 \lesssim 1.3$); whether the wall is flat or curved, it is an experimental fact under these conditions that the resulting interaction flow pattern is of the relatively-simple type* illustrated in Fig. 2A. The boundary layer spreads out the shock perturbation upstream as well as downstream to give a wall pressure distribution such as shown in Fig. 2B. There is observed a corresponding significant local

---

* When separation occurs, this pattern changes rapidly to a much more complicated one involving a bifurcated shock structure[4].

growth of the boundary layer displacement thickness, particularly behind the shock (Fig. 2C), so that even though the original undisturbed boundary layer is thin and negligibly affects the overlying inviscid flow, this is no longer the case in the interaction zone astride the shock whether or not the wall is flat.

Thus, the local outer inviscid flow "sees" the overall viscous effects in the interaction as an effective thickening of the geometrical surface by an amount equal to the interactive displacement thickness growth. In the vicinity of the shock, this is seen to involve (a) a rapid growth in the effective body slope at the shock foot followed by (b) an overall downstream increase of the effective body thickness. At the very least, these two features must be included in any realistic mathematical model of the true outer inviscid flow in such interactions.

3. OUTER INVISCID FLOW MODEL

Consider the local mixed inviscid transonic flow in the neighborhood of the shock outside the boundary layer, assuming the shock weak enough to be isentropic. Then if W and ϑ are the magnitude and direction angle, respectively, of the resultant flow velocity and we introduce the transformed dependent variables

$$S = \pm \frac{3}{2} (\gamma+1)^{1/2} \cdot \sigma^{-1} \left(\frac{W}{a^*} - 1 \right)^{3/2} \tag{1a}$$

$$t = \sigma^{-1} \vartheta \tag{1b}$$

as functions of the stretched independent variables

$$X = x \tag{2a}$$

$$Y = \left[\frac{3}{2} (\gamma+1)\sigma \right]^{1/3} y \tag{2b}$$

where the constant σ is chosen later as an appropriate similarity parameter, then the governing transonic flow equations are:

$$S^{1/3} \frac{\partial S}{\partial X} - \frac{\partial t}{\partial Y} = 0 \tag{3a}$$

$$S^{-1/3} \frac{\partial S}{\partial Y} \mp \frac{\partial t}{\partial X} = 0 \tag{3b}$$

This pair of equations in general has either supersonic wave-type solutions ($S > 0$, minus sign in 3b) or subsonic Cauchy - Riemann - type solutions ($S < 0$, positive sign). If we further restrict attention to small perturbations about the shock conditions, Eqs. (3) become linear in the leading approximation.

We now choose σ such that upstream of the shock $S = S_1 = 1$; then linearization of Eq. (3) gives a wave equation with solutions of the form[7]

$$S = S_1 + F_1(\xi) + G_1(\eta)$$
$$t = t_1 + F_1(\xi) - G_1(\eta) \tag{4}$$

where $\xi = X + Y$ and $\eta = X - Y$. We linearize the subsonic equations for perturbations of the post-shock condition $S_2 < 0$, t_2 and find the solution of the Cauchy-Riemann equations[7]:

$$Z = X + iS_2^{1/3}Y$$
$$= S_2 + it_2 + F_2(Z) \tag{5}$$

A particular case of a pair of local solutions (4) and (5) pertains to the flow ahead and behind an oblique shock of the "strong branch" type, i.e., with subsonic flow downstream. The transonic shock jump conditions link the pre- and post-shock conditions as follows:

$$\Delta t = t_2 - t_1 = 2^{-3/2} \cdot 3 \cdot (1 - S_2^{2/3})^{1/2} (1 + S_2^{2/3}) \tag{6a}$$

$$\text{Ctg } \beta = 2^{-5/6} \cdot 3^{1/3} (\gamma + 1)^{1/3} \sigma^{1/3} (1 - S_2^{2/3})^{1/2} \tag{6b}$$

Thus, if at some point P there is a supersonic flow $W_1 > a^*$ at inclination V_1 that is decelerated by an oblique shock to some $W_2 < a^*$ at angle ϑ_2 (Fig. 3A) then $W_1, \vartheta_1, W_2, \vartheta_2$ are related in terms of S_1, t_1, S_2, t_2 by means of

Eqs. (1a, 1b, 6a). This is the transonic shock polar (Fig. 3b) and we find the wave angle β corresponding to the flow deflection angle* from Eq. (6b). Then with given shock jump conditions at P, the local solutions (4) and (5) may be used to determine the velocity gradients as well as the curvature of the shock shape in the vicinity of P.

This local transonic inviscid perturbation field now can be linked to the inner viscous disturbance flow by noting from above that the outer flow sees an effective body consisting of the bare wall $h_w = h_1 = C_1 X^2$ plus a slope jump C_2 at the shock foot followed by a further interactive displacement thickness growth, giving $h_2 = h_{w,eff} = C_2 X + D_2 X^2$ (see Fig. 4a). Upstream of the shock, an arbitrary linear variation of inviscid flow Mach number along the wall is assumed (Fig. 4b) to allow for either decelerating, accelerating or uniform incoming supersonic flow. Now in terms of this flow model, a local analytic solution can be carried out[7] by a double series expansion analysis** of the upstream and downstream flow properties about the shock-foot origin using the following particular solutions of Eqs. (4) and (5):

$$F_1 = A_1 \xi$$

$$G_1 = B_1 \eta \qquad (7)$$

$$F_2 = A_2 Z + B_2 Z \ln Z$$

The downstream (complex) coefficients A_2, B_2 are related to their upstream (real) counterparts and the shock shape parameters by the transonic shock polar. The result of this analysis yields two basically different types of physical

---

* It is assumed here that the deflection angle $\vartheta_2 - \vartheta_1$ lies below the maximum value of the shock polar, which is reasonable in practice if the incident shock is weak enough to avoid separation.

** The realistic assumption is made here that the radius of any wall curvature is large compared with a typical boundary layer displacement thickness.

behavior (one regular, the other singular) depending on whether the interactive deflection effect is included ($C_2 > 0$, $D_2 \neq C_1$) or neglected a priori ($C_2 = 0$, $D_2 = C_1$),as follows.

(1) $C_2 > 0$, $D_2 \neq C_1$

Regular Solution F_2: $A_2 \neq 0$, $B_2 = 0$ (8a)

Parabolic Oblique Shock Shape: $X_{sh} = Qy + Py^2$ (8b)

Linear Downstream Wall Pressure: $M_2-1 = K_2 + L_2X$ (8c)

as typically illustrated in Fig. 4b (expressions for P, Q, K_2, L_2 are given in the Appendix). Owing to the displacement thickness effect, note here that the inviscid normal shock actually is curved near the boundary layer edge with a slightly oblique angle at the foot.[9]

(2) $C_2 = 0$, $D_2 = C_1$

Singular Solution F_2: $A_2 = 0$, $B_2 \neq 0$ (9a)

Curved Shock Normal to Wall: $X_{sh} = y^2 (Q + R \ln y)$ (9b)

Logarithmically Singular Pressure: $M_2=-K_1 (1-E_2X-F_2X \ln X)$ (9c)

as schematically depicted in Fig. 5 (the appropriate coefficients can be found in Ref. 8.) This "bare" curved wall solution is in fact the Oswatitsch-Zierep singular solution[1] mentioned earlier. It has been of use mainly to verify computational results for inviscid flows with recompression shocks: fully conservative codes usually give results with a post-shock expansion, demonstrating the locally-exact treatment of the recompression shock if the computational grid is fine enough[3].

The authors of Ref. 1 were inspired to clarify the problem of the normal shock on a curved wall by Ackeret's remarks about an experimentally-observed[4]

sharp post shock expansions at the boundary layer edge. But these were observed for laminar boundary layer interactions where a lambda shock configuration occurs and an expansion fan follows the strong main shock sitting on a large separation bubble (Fig. 6). For the experiments with turbulent boundary layer interaction[4] without separation, however, this does not occur; instead, an oblique shock shape occurs on a ramp-like thickening of the turbulent boundary layer[7]. From these observations we conclude that the singular solution involving the logarithmic terms (Eqs. 9) might be applicable in modeling the outer flow near the shock foot in the case of a fully-separated flow where the "wall" shape is given by the curved separation bubble geometry and not by the underlying solid wall (although in this situation, shock reflection is governed by a free streamline instead of a solid wall boundary condition so that a singularity still need not necessarily occur). However, for non-separating turbulent boundary layer interactions, the regular solution (8) is the appropriate inviscid flow model even on a curved wall because it takes into account the flow deflection and shock distortion due to the interaction-induced boundary layer thickening. Thus the turbulent interaction outer flow model is primarily determined by the deflection ramp and not by wall curvature; curvature does have some influence (as we show below) but it is regular and does not derive from any singular behavior in the inviscid part of the flow. This conclusion is concordant with all known theory and experiment on viscous-inviscid interactions in general: coupling of the inviscid flow with the interactive displacement effect invariably eliminates local mathematical singularities that otherwise may occur in solving the flow equations.

The foregoing discussion shows that Eqs. (8) are the correct mathematical model of the local interacting inviscid flow near the shock including any surface curvature. As indicated in the Appendix, the downstream solution

coefficients C_2, D_2, K_2, L_2 are related to the upstream coefficients C_1, K_1, L_1 and those of the shock shape (P,Q) by four equations; since the basic wall shape (C_1) and incoming supersonic flow (K_1, L_1) are usually known in practice, any pair of the remaining coefficients must be given to determine the others. This implies three possibilities: (a) a prescribed shock shape (P,Q) based on a Schlieren photo, leading to the corresponding effective interactive wall shape and downstream flow; (b) a given post-shock Mach number distribution (K_2, L_2) obtained from wall pressure data, leading to the corresponding shock and effective wall shapes; (c) a known post-shock displacement effect (C_2, D_2) given either by measurement or an interactive boundary layer theory, leading to the outer shock shape and inviscid pressure distribution. Here we are concerned with (c); further discussion of the others is given elsewhere[8,10].

4. INNER VISCOUS FLOW MODEL

4.1 General Features

The present treatment of the interactive perturbation field within the inner turbulent boundary layer region is based on an appropriate extension of Inger and Mason's approximate analytical theory[11] to include consideration of wall curvature effects. Consider a known adiabatic boundary layer profile $M_o(y)$ subjected to small transonic disturbances due to an impinging weak and nearly normal shock. In the practical Reynolds number range of interest here ($10^5 \leq Re_L \leq 10^8$), we employ a non-asymptotic disturbance flow model in the turbulent boundary layer patterned after the Lighthill-Stratford-Townsend double-deck approach[23,24] that has proven highly successful in treating a variety of other problems involving turbulent boundary layer response to strong rapid adverse pressure gradients. This was done because of the large body of turbulent boundary layer-shock interaction data that strongly supports such a model in this

Reynolds number range[25,26] (including the present transonic regime) and the findings of a separate general theoretical study[27] suggesting that the results of the asymptotic theory approach for very high Reynolds numbers,[20,28] although rigorous in this limit, may not extrapolate down to the present Reynolds number range.

The resulting flow model consists of an inviscid boundary value problem surrounding a nonlinear shock discontinuity and underlaid by a thin viscous disturbance sublayer as schematically illustrated in Fig. 7. An approximate analytical solution is further achieved in the leading approximation by introducing some engineering simplifications[11] (including the assumption of small linearized disturbances ahead of and behind the nonlinear shock jump plus neglect of the detailed shock structure within the boundary layer[12]) which have been shown to give accurate results for the overall properties of engineering interest provided M_1 is not too close to unity ($M_1 \gtrsim 1.05^*$). This yields a triple-deck solution consisting of (a) linearized potential supersonic disturbance flow in region 1 plus the subsonic disturbance flow in region 3 caused by the interaction-generated interface displacement $\eta_3(x)$ and the post-shock perturbations along $x = 0^+$ due to the impongement of region 1 Mach wave disturbances on the shock; (b) underneath, a rotational inviscid disturbance flow region 2 in the boundary layer; (c) a thin viscous disturbance sublayer[13] within the linear part of the basic velocity profile $U_o = (\tau_w/\mu_w)y$ which carries most of the upstream influence of the interaction. A known solution for this sublayer[13] can be extended to the present

---

* As far as the overall interaction solution for $10^5 \leq Re_L \leq 10^8$ is concerned, the nonlinear shock jump conditions plus the non-uniform viscous flow effects in the boundary layer reduce the lower Mach number limit otherwise pertaining to the linearized supersonic theory in purely inviscid potential flow (see Ref. 21 for more detailed discussion).

problem to obtain the displacement effect (effective wall position seen by the overlying rotational inviscid disturbance flow) and also the corresponding disturbance skin friction caused by the pressure disturbance field.

The matching of these regional solutions yields linear integral equations that can be solved by operational methods for the disturbance pressure along both the boundary layer edge and wall[11]. The remaining interactive flow properties can then be determined in terms of p'_w, including the interactive growth in displacement thickness and the corresponding skin friction perturbation. It is noted that this latter perturbation solution has been extended downstream as well as upstream of the shock and further corrected for the nonlinear inertia effects in an adverse pressure gradient using the general non-dimensional wall shear-pressure solution ahead of separation given by formal triple deck theory[5]; when converted to turbulent flow by expressing all results in terms of C_{f_o} instead of Re_L, this yields

$$C_f(x) \simeq C_{f_o} - \sqrt{\beta C_{f_o}\left[1 + \left(\frac{C_f(x) - C_{f_o}}{1.234 C_{f_o}}\right)\right]}\; C'_{p_w}\; F(x/\delta_o) \qquad (10)$$

where the non-dimensional function F is essentially unity ahead of the shock $x < 0$ and vanishes slowly behind it with $F \sim (x/\delta_o)^{-1/3}$ far downstream. It is seen from Eq. (10) that depending on Reynolds number (C_{f_o}), a sufficiently strong interactive pressure rise can cause incipient separation ($C_f \to 0$) near the shock.

This flow model contains all the essential global features of the mixed transonic character of the non-separating normal shock-turbulent boundary layer interaction problem including the significant lateral pressure gradient effects, upstream influence and interactive skin friction for an arbitrary input turbulent boundary layer profile. Detailed comparisons with experiment[14,15] have shown that it gives a very good account of all the important engineering features of

the interaction over a wide range of Mach-Reynolds number conditions at very low computational cost. Hence the theory provides a sound basis for interpreting experimental data on unseparated flow and for further extensions to account for slight wall curvature.

It is noted that this solution in principle may be used with a mean turbulent boundary layer profile input from either experimental measurement or any theoretical prediction method. Here we have chosen an approximate but accurate and particularly convenient analytical profile model by LeFoll that is in frequent use in boundary layer studies, has considerable parametric generality and proves especially well-suited to perturbation problems in non-uniform flows (a detailed description may be found elsewhere[16, 17]). It is characterized quite generally by three parameters (M_1, boundary layer thickness Reynolds number and the incoming shape factor) and readily permits the introduction of the effects of wall curvature as shown below.

4.2 Longitudinal Curvature Effects

Now wall curvature influences the inner solution in two ways: (1) it alters the incoming undisturbed turbulent boundary layer profile upon which the perturbation solution depends; (2) it introduces new explicit terms in the small disturbance equations. The first is by far the most important and is discussed further below; the secondary effects (2) are in fact negligible for the small relative curvatures ($\delta_o/R_B \leq .02$) encountered in practice according to the following considerations. As regards the (regular) influence of curvature on the inviscid outer boundary conditions via the displacement effect, the foregoing analysis shows that this is of order δ_o^*/R_B and hence very small in the leading approximation. Likewise, under the continued assumptions that the interactive disturbances remain uncorrelated with the background turbulent fluctuation field

and that the viscous disturbance sublayer lies within the laminar sublayer region of the turbulent boundary layer, the new terms in both the rotational inviscid and viscous disturbance sublayer equations can be shown[16] to be of the same order or smaller and hence also negligably small. Thus, to a consistant degree of first approximation, the form of the equations governing the disturbance flow in the boundary layer is not altered by wall curvature.

Regarding the basic turbulent flow profile, once again the explicit new curvature terms in the flow equations governing this profile (including the centrifugal lateral pressure gradient effect) have all been shown to be of the order δ_o/R_B and hence negligible (e.g., see Bradshaw's monograph[18] and more recent work[19]). However, the influence on the eddy viscosity relation is known to have an order of magnitude larger effect (10 to 20 * δ_o/R_B) on the overall skin friction τ_{w_o} and form factor H_i (Ref. 18); since it has been firmly established that the role of the profile in the interaction mainly derives from these properties[17], this influence is therefore the cause of any significant curvature effect on the interaction solution.

By virtue of the foregoing arguments, the curvature effect can be reasonably estimated by incorporating into the incoming boundary layer profile model appropriate corrections for the influence of curvature on C_{f_o}, the form factor and thickness. Examination of Bradshaw's comprehensive study [18] shows that over a wide range of parametric and local conditions, these corrections for small longitudinal curvature and non-separating flows can be represented by the engineering approximations*

---

* It is emphasized that the use of a more detailed, sophisticated model will not alter the general trends and qualitative conclusions of primary concern here.

$$C_{f_o} \simeq \left(1 - 10\,\frac{\delta_o}{R_B}\right) \cdot \left(C_{f_o}\right)_{flat} \tag{11a}$$

$$H_{i_1} \simeq \left(1 + 5\,\frac{\delta_o}{R_B}\right) \cdot \left(H_{i_1}\right)_{flat} \tag{11b}$$

where to this first order accuracy the corresponding effect on δ_o is much smaller and therefore neglected. Note that the typical value $\delta_o/R_B \approx .01$ yields a reduction and increase in C_{f_o} and H_{i_1} of 10% and 5%, respectively, which are an order of magnitude larger than the explicit new curvature terms in either the mean or perturbation flow equations (including the outer inviscid disturbances). The use of Eqs. (11) with δ_o/R_B as an additional input parameter in the Inger-Mason-Panaras theory[11,17] enables a straightforward appraisal of the first order curvature effects on the non-separating normal shock-turbulent boundary layer interaction problem. The results of such a study will now be presented.

5. DISCUSSION OF RESULTS

5.1 Parametric Study

The typical influence of curvature on the interactive wall pressure distribution is illustrated in Fig. 8; the corresponding displacement thickness growth and local skin friction behavior are shown in Figs. 9 and 10. Fig. 8 shows that the curvature effect from C_{f_o} has a very small influence (this in fact was found to be true over a wide range of M_1 - Re_L conditions), whereas that from the form factor is of controlling importance. Since curvature increases H and hence reduces the incoming profile "fullness", it acts to spread out the wall pressure disturbance,[17] increase the upstream influence, reduce the downstream pressure level and (Fig. 9) thicken the downstream boundary layer. The corresponding influence on skin friction (Fig. 10) is especially significant:

although curvature reduces the upstream level, it increases the local C_f near the shock foot owing to the reduced adverse pressure gradient. Thus wall curvature retards the onset of incipient separation that tends to occur slightly downstream of the shock*.

The curvature effect on the pressure disturbance along the outer edge of the boundary layer (Fig. 11) is also of interest and brings out several fundamental points. First, a small subsonic expansion region is predicted to occur right behind the shock regardless of the wall curvature; this was shown to be an inherent feature of the mixed transonic viscous interaction flow along a flat surface by Inger and Mason[11] and is further confirmed by detailed numerical solutions[20]. Thus, contrary to what is sometimes alleged, wall curvature per se is not the cause of such expansion regions in non-separating turbulent interactions. Second, when horizontal distance is properly rescaled so that $x \sim 0\ (\delta_0)$ as is done in Fig. 11, these regions are perfectly regular as predicted by Eqs. (8). Third, although not the cause, convex wall curvature does strengthen the expansion and reduce the preceding local shock pressure jump. We re-emphasize, however, that this is a result of the curvature effect on the boundary layer eddy viscosity and has nothing whatsoever to do with any inviscid curvature singularity.

5.2 Comparison with Experiment

Ackeret, Feldman and Rott's famed experimental study[4] of shock-boundary layer interaction on a plate and wall in the choked transonic flow of a slightly-curved wind tunnel nozzle provides some examples of unseparated turbulent flow

* Although the skin friction solution of the present theory is no longer valid for separated flow [$C_f(x) < 0$ over some portion of the wall] it is still useful to indicate trends toward this situation, i.e., where and when incipient separation ($C_f \to 0$ at some x) first occurs.

suitable for comparison with the present theory. We have chosen those for which both wall and inviscid pressure distributions, as well as displacement thickness, are given.

It is noted that direct comparisons with these data involve numerous uncertainties in converting to the theoretical variables (or vice-versa). (a) the boundary layer thickness and hence the inviscid flow edge is only approximately defined; (b) the shock wave location and shape are uncertain to within .25 to .50 $\times \delta_o$; (c) reading the curves where they change rapidly introduces inherent error; (d) a significant background inviscid pressure gradient is present which beclouds interpretation of the outer fringes of the interaction zone and the character of the incoming "undisturbed" turbulent layer profile; (e) the upstream boundary layer history is only partially understood, especially following forced transition cases, and this together with (d) cannot be fully accounted for in the local interaction model; (f) a significant channel blockage effect occurs from the interactive boundary layer thickening, which reduces the effective theoretical shock strength and hence the downstream interaction pressure level (this was first identified independently by Inger and Panaras[16, 17] and Melnick and Grossman[22] who devised different but equivalent correction methods for it).

A typical non-separating interactive pressure field measured by AF & R[4] is illustrated in Fig. 12a; experimental pressure distributions along both the surface and the approximate boundary layer edge are compared in Fig. 12b with the theoretical prediction (corrected for the estimated interactive blockage effect using the Inger-Panaras method)[17], while the corresponding displacement thicknesses are shown in Fig. 12c. We note that the relevant non-dimensional curvature parameter for these experiments was rather small ($K \cdot \delta_o \simeq .0063$) so that the predicted curvature effect on the interaction is only slight, as indicated. In view of the aforementioned uncertainties in

interpreting the data plus the limitations of the theory (e.g., the small disturbance approximations and neglect of the detailed nonlinear wave diffraction effects in the supersonic portion of the boundary layer), the overall agreement is seen to be quite good. In particular, the following definitive features of the interaction predicted by the theory are well-corroborated: (1) the magnitude, sign and streamwise extent of the lateral pressure gradient effect both ahead and behind the shock; (2) the existence of a long slow interactive pressure rise (algebraic rather than exponential) downstream of the shock; (3) the overall streamwise scale and upstream influence distance; (4) the magnitude and shape of the interactive displacement thickness growth; (5) the local inviscid pressure jump across the shock at the boundary layer edge; (6) a non-singular inviscid subsonic expansion region behind the shock due to the viscous-inviscid interaction and not surface curvature (note that the zero curvature theory in this region is actually closer to the data), consistent with the regular inviscid post-shock model.

From foregoing results it is concluded that the inviscid regions of sharp pressure rise followed by expansion typified by Fig. 12a should not be physically interpreted as a symptom of an inviscid curvature singularity but rather as inherent features of the viscous mixed transonic interaction that occur even on a flat surface and which are only secondarily-influenced by curvature.

6. CONCLUDING REMARKS

This investigation has sought to delineate the essential influence of surface curvature on non-separating turbulent boundary layer-transonic shock interactions, to place in true perspective the inviscid curvature singularity, and to devise an approximate analysis including curvature that enables both parametric study and comparisons with experiment. The resulting theory is in

fact tatamount to a non-asymptotic triple deck model of the interaction pertaining to the Reynolds number range $10^5 \leq Re_L \leq 10^8$. Although it may therefore be improved upon by a more rigorously-detailed treatment the primary results should remain the same, including the following overall qualitative conclusion: when the viscous displacement effect on the inviscid flow is accounted for (as it must by very definition of an interaction problem), the surface curvature effect on non-separating interactions is non-singular and derives from its influence on the eddy viscosity within the boundary layer.

APPENDIX

Determination Of Solution Coefficients For Transonic Flow Past A Ramp Streamline With Compression Shock (Ref. 24)

We refer to Eqs. (6) - (8) plus Figs. 3 and 4; it is assumed that the following coefficients are known: C_1 (solid wall curvature), K_1 (pre-shock Mach number), L_1 (pre-shock acceleration), C_2 (post-shock streamline inclination at boundary layer edge) and D_2 (post-shock streamline curvature at boundary layer edge). Then in terms of the auxilary formulae

$$\mu = 3L_1/(2K_1) \tag{A-1}$$

$$\nu = 3 \cdot 2^{-3/2} (\gamma + 1) K_1^{-3/2} \cdot C_1 \tag{A-2}$$

$$\omega = 3 \cdot 2^{-3/2} (\gamma + 1) K_1^{-3/2} \cdot C_2 \tag{A-3}$$

$$\Delta t = 2^{-5/2} \cdot 3 \cdot (\gamma + 1) C_2 K_1^{-3/2} \tag{A-4}$$

inversion of the transonic shock polar (Fig. 3B) on the strong shock branch ($-1 \leq S_2 \leq -3^{-3/2}$) gives

$$S_2 = - [(1 - 3^{-3/2}) \sqrt{1 + a \cdot \Delta t^2 + b \cdot \Delta t^4 + c \cdot \Delta t^6} + 3^{-3/2}] \tag{A-5}$$

where for $\gamma = 1.40$, $a = -0.8255$, $b = 0.0$, $c = 0.0425$. Further, the desired unknown coefficients take the following values:

$$P = 2^{1/2} K_1^{1/2} (1 - S_2^{2/3})^{1/2} \text{ [compression shock inclination]} \tag{A-6}$$

$$Q = \xi \cdot \lambda \cdot K_1 \text{ [compression shock curvature]} \tag{A-7}$$

$$K_2 = -S_2^{2/3} \cdot K_1 \text{ [post-shock Mach number]} \tag{A-8}$$

$$L_2 = 2 \rho K_2 / 3S_2 \text{ [post-shock acceleration]} \tag{A-9}$$

where

$$\xi = \sqrt{1 - S_2^{2/3}} \tag{A-6}$$

$$\eta = \xi S_2^{-1/3} (4\xi^2 - 5 S_2^{2/3} - 1) \tag{A-7}$$

$$\zeta = 8\xi^2 - S_2^{2/3} - 1 \tag{A-8}$$

$$\tau = \mu\xi[4(1 + \xi^2) + S_2^{2/3} + 1] + (8 \xi^2 + S_2^{2/3} + 1) \tag{A-9}$$

$$\rho = (\zeta\omega - \tau)/\eta \tag{A-10}$$

$$\lambda = [\xi(\mu - \rho \cdot S_2^{-1/3}) + \omega + \nu] / 3(1 - S_2^{2/3}) \tag{A-11}$$

REFERENCES

1. Oswatitsch, K. and J. Zierep, "Das Problem des senkrechten Stosses an einer gekrümmten Wand", ZAMM 40 (1960), pp. 143.
2. Emmons, H. W., "Theoretical Flow of a Frictionless Adiabatic Perfect Gas Inside a Two-Dimensional Hyperbolic Nozzle", NACA TN-1003, 1946.
3. Jameson, A., "Iterative Solution of Transonic Flows Over Airfoils and Wings," Comm. Pure Appl. Math., Vol. 27, 1974, pp. 283-309.
4. Ackeret, J., F. Feldman and N. Rott, "Investigation of Compression Shocks and Boundary Layers in Gases Moving at High Speed", NACA TN-1113, 1947.
5. Stewartson, K. and P. G. Williams, "Self-Induced Separation", Proc. Royal Soc. A 312, 1969, pp. 181-206.
6. Bohning, R. and J. Zierep, "Der Senkrechte Verdichtungs-Stoss an der gekrümmten Wand unter Berücksichtigung der Reibung", ZAMP 27 (1976), pp. 225-240.
7. Sobieczky, H., "Die Struktur der Aussen-Strömung bei Transsonischer Stoss-Gienzschicht Interferenz", Deutsche Forschungs-und Versuchsanstalt für Luft-und Raumfahrt Report IB 251-76A15, Göttingen, Sept. 1976.
8. Sobieczky, H., "A Computer Program for Analysis of Transonic Flows Past a Wall Ramp", Engineering Experiment Station, College of Engineering, The University of Arizona, Tucson, June, 1978.
9. Inger, G. R. and H. Sobieczky, "Shock Obliquity Effect on Transonic Shock-Boundary Layer Interaction", ZAMM 58T, 1978.
10. Sobieczky, H. and E. Stanewsky, "The Design of Transonic Airfoils Under Consideration of Shock Wave-Boundary Layer Interaction", ICAS Paper 76-14, Ottawa, 1976.
11. Inger, G. R. and W. H. Mason, "Analytical Theory of Transonic Normal

Shock-Turbulent Boundary Layer Interaction", AIAA Journal 14, May 1976, pp. 1266-72.

12. Inger, G. R., "Shock Penetration and Lateral Pressure Gradient Effects on Transonic Viscous Interactions", AIAA Journal 15, Aug. 1977, pp. 1198-1200.
13. Lighthill, M. J., "On Boundary Layers and Upstream Influence, II. Supersonic Flow without Separation", Proc. Royal Soc. A 217, 1953, pp. 478-507.
14. Inger, G. R., "Theoretical Study of Reynolds Number and Mass Transfer Effects on Normal Shock-Turbulent Boundary Layer Interaction", Zeitschrift für Flug-und Raumfahrt Wissenschaften (to be published).
15. Inger, G. R., "Analysis of Transonic Normal Shock-Boundary Layer Interaction and Comparisons with Experiment", AIAA Paper 76-331, July 1976 (VPI&SU Report Aero-053, Blacksburg).
16. Panaras, A. G., "Normal Shock-Boundary Layer Interaction in the Presence of Streamwise Pressure Gradient", Ph.D. Thesis, Univ. Libre de Bruxelles, 1976 (Von Karman Institute Report).
17. Panaras, A. G. and G. R. Inger, "Transonic Normal Shock-Turbulent Boundary Layer Interaction in Pressure Gradient Flows", ASME Paper 77-GT-34, March 1977.
18. Bradshaw, P., "Effects of Streamline Curvature on Turbulent Flow", Agardograph 169, Aug. 1973.
19. So, R. M. and G. L. Mellor, "Turbulent Boundary Layers with Large Streamline Curvature Effects", ZAMP 29, 1978, pp. 54-74.
20. Melnick, R. E. and B. Grossman, "Analysis of the Interaction of a Weak Normal Shock Wave with a Turbulent Layer", AIAA Paper 74-598, June 1974.

21. Mason, W. H. and G. R. Inger, "Analytical Study of Transonic Normal Shock-Boundary Layer Interaction", AIAA Paper 75-831, June 1975.

22. Melnick, R. E. and B. Grossman, "Further Developments in an Analysis of the Interaction of a Weak Normal Shock Wave with a Turbulent Boundary Layer", Proc. Symp. Transonicum II, Springer-Verlag, 1976, pp. 262-72.

23. Stratford, B. S., "The Prediction of Separation of the Turbulent Boundary Layer", Jour. Fluid Mech. 5, pp. 1-16, 1959.

24. Townsend, A., "The Behavior of a Turbulent Boundary Layer Near Separation", Jour. Fluid Mech. 12, pp. 536-554, 1967.

25. Green, J. E., "Interactions Between Shock Waves and Turbulent Boundary Layers", Von Karman Inst. Report LS-10, Brussels, Jan. 1969.

26. Rose, W. C. and D. A. Johnson, "Turbulence in Shock-Wave Boundary Layer Interaction", AIAA Jour. 13, pp. 884-889, July 1975.

27. Inger, G. R., "Upstream Influence in Interacting Non-separated Turbulent Boundary Layers", paper presented at the Workshop on Viscous Interaction and Boundary Layer Separation, Ohio State Univ., Columbus, Aug. 17, 1976 (VPI&SU Report in preparation).

28. Adamson, T. C. and A. Feo, "Interaction Between a Shock Wave and a Turbulent Boundary Layer in Transonic Flow", SIAM Jour. of Applied Math. 29, 1975.

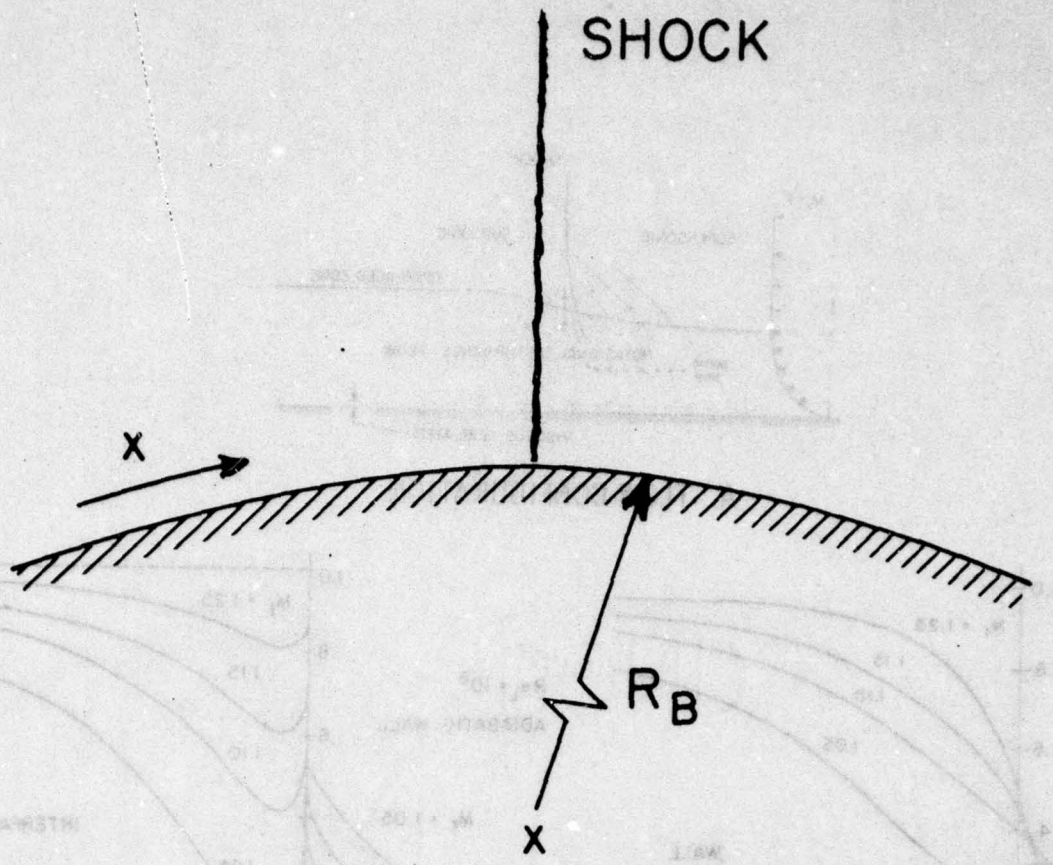

Fig. 1 Inviscid Shock on a Curved Wall (Schematic)

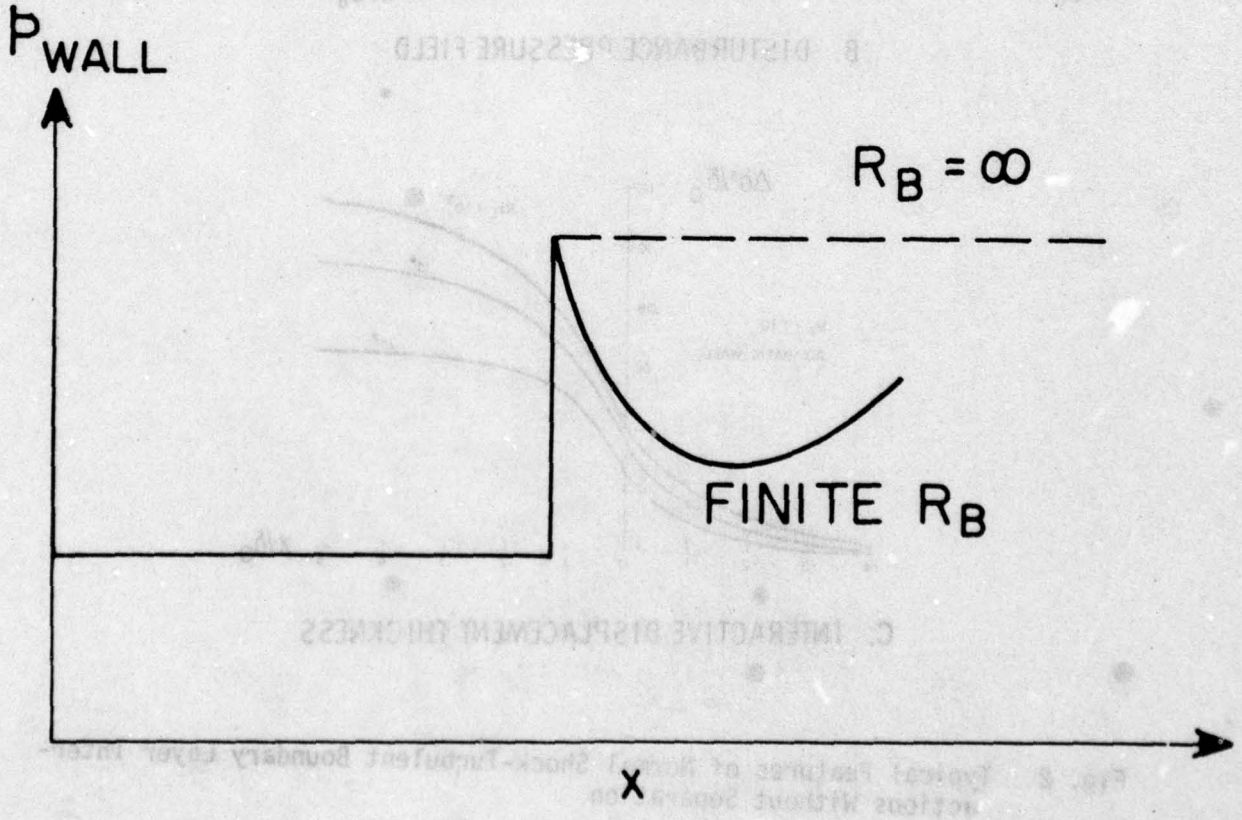

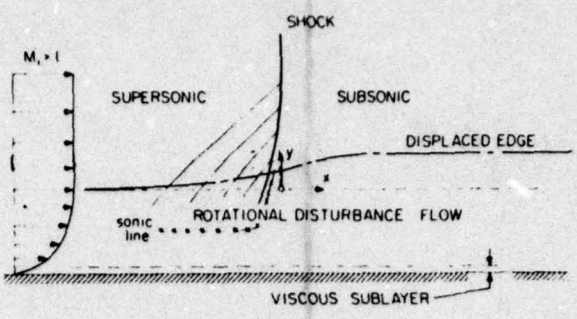

A. FLOW CONFIGURATION

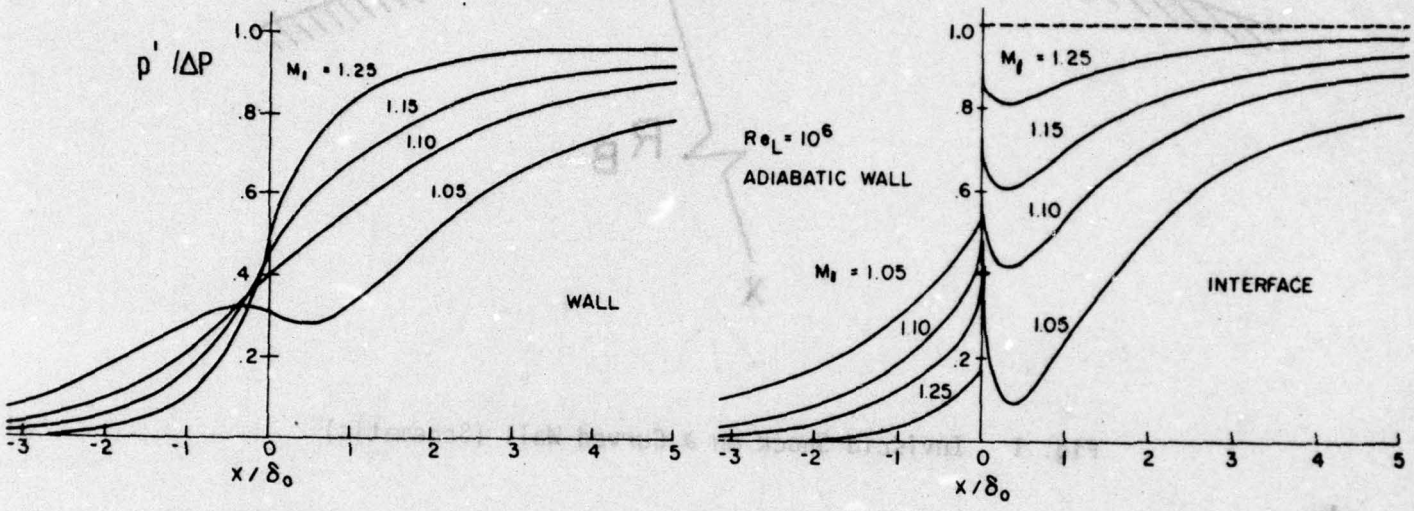

B. DISTURBANCE PRESSURE FIELD

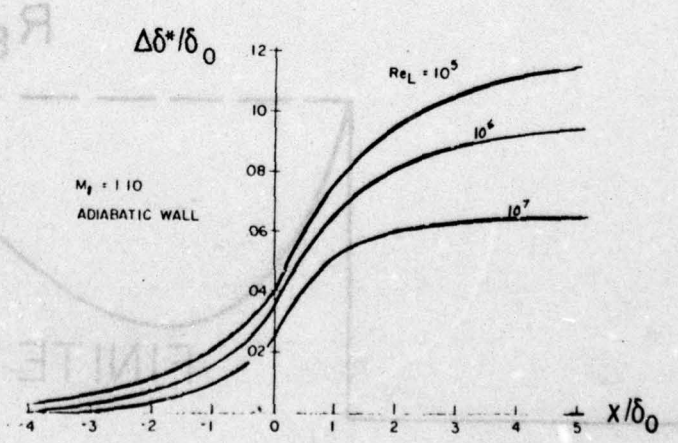

C. INTERACTIVE DISPLACEMENT THICKNESS

Fig. 2 Typical Features of Normal Shock-Turbulent Boundary Layer Interactions Without Separation

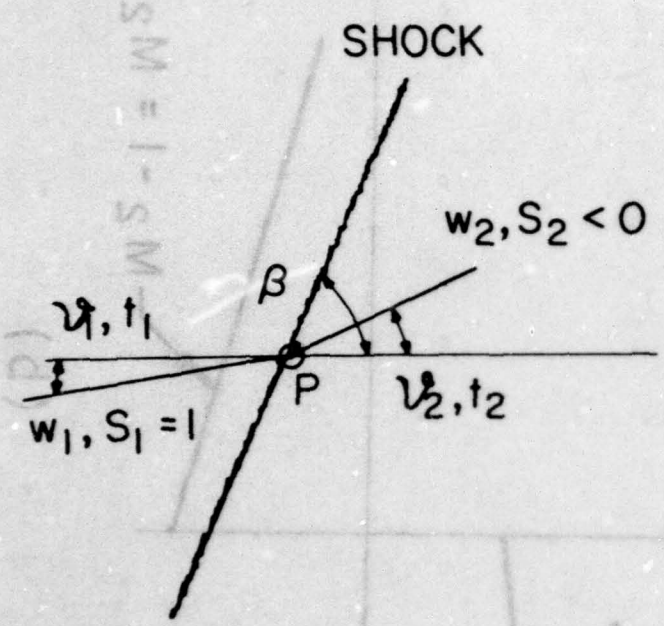

(a)

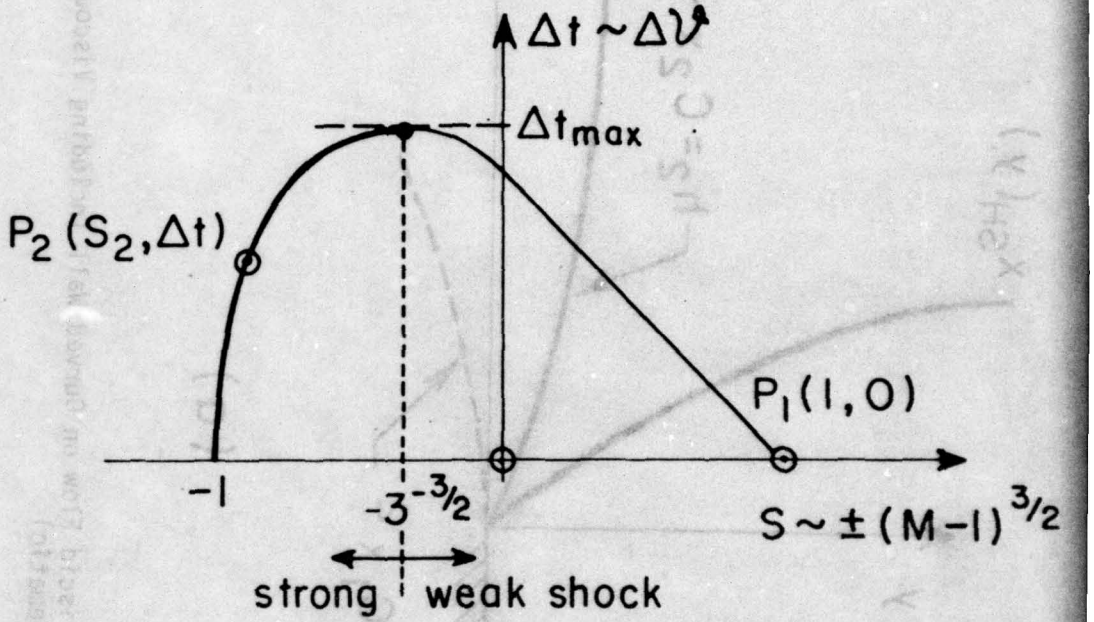

(b)

Fig. 3 Shock Polar Diagram

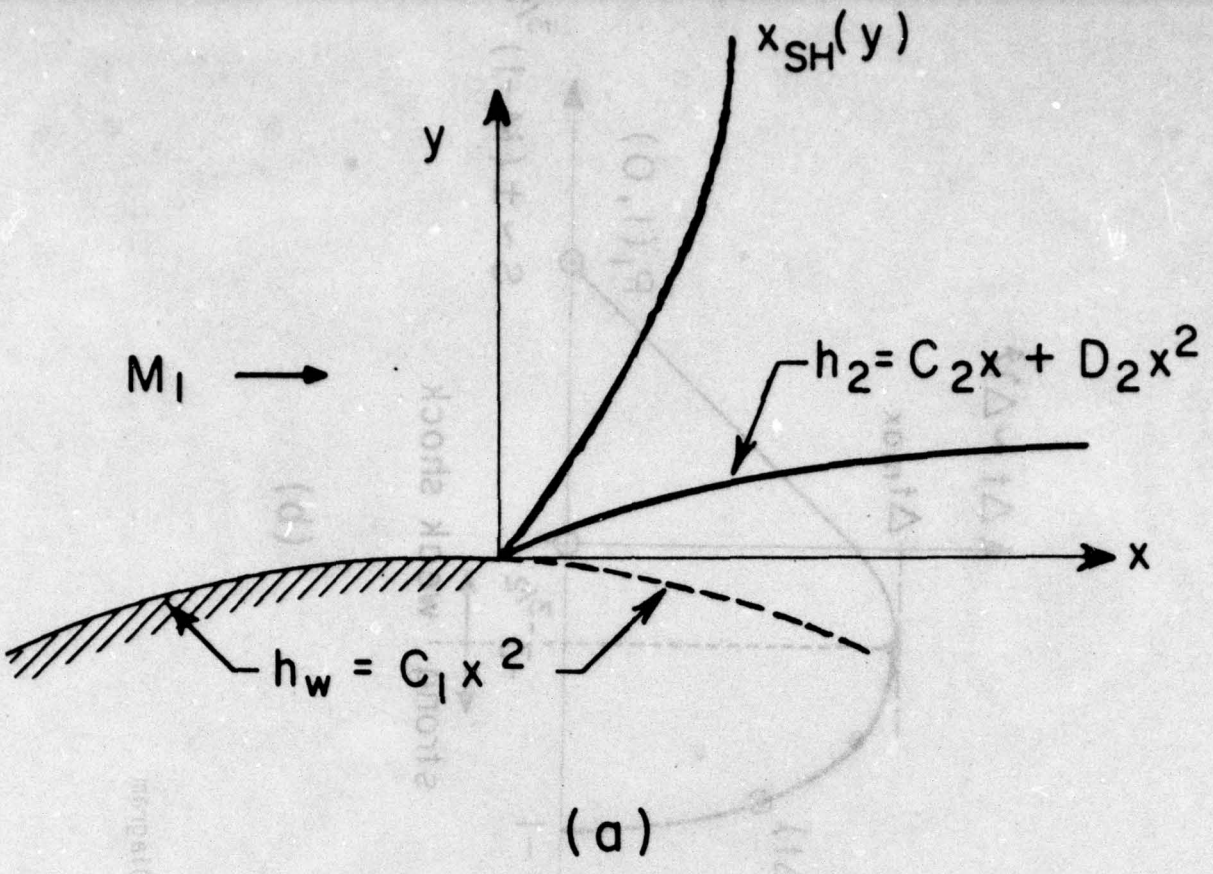

Fig. 4 External Inviscid Flow on Curved Wall Including Viscous Displacement Effect (Schematic)

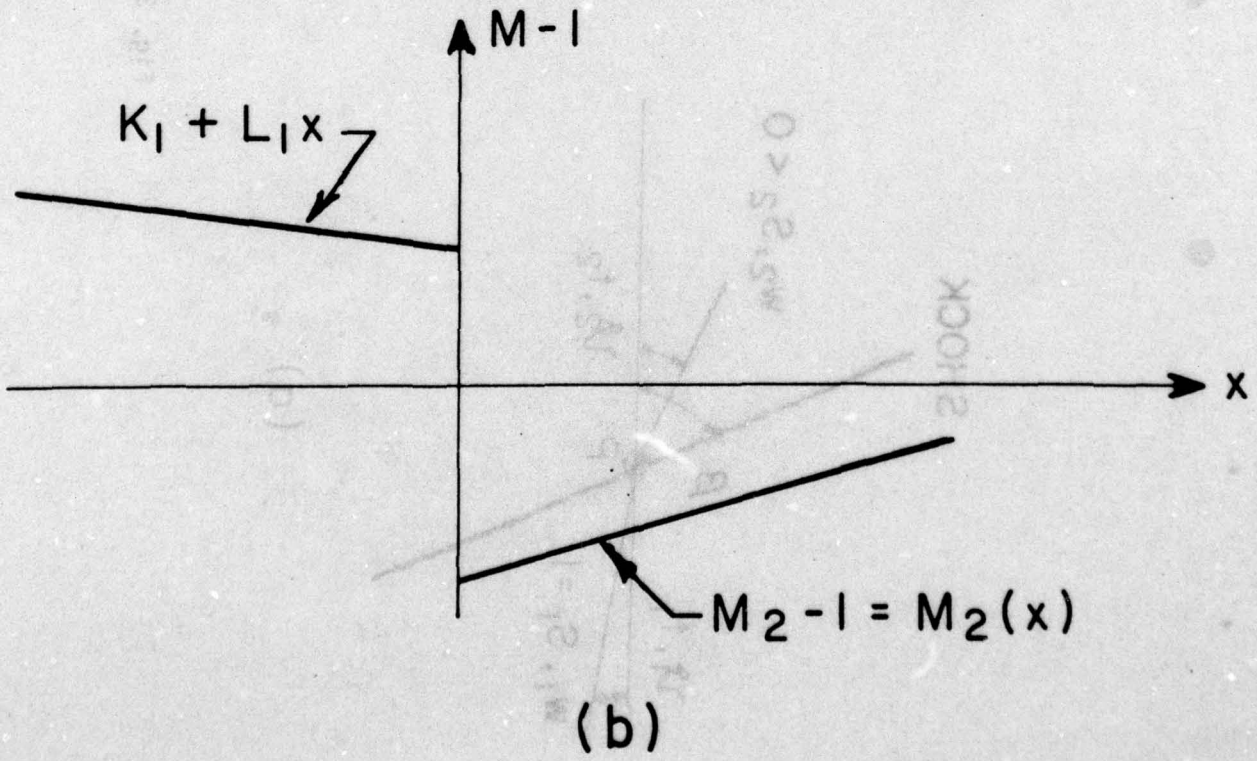

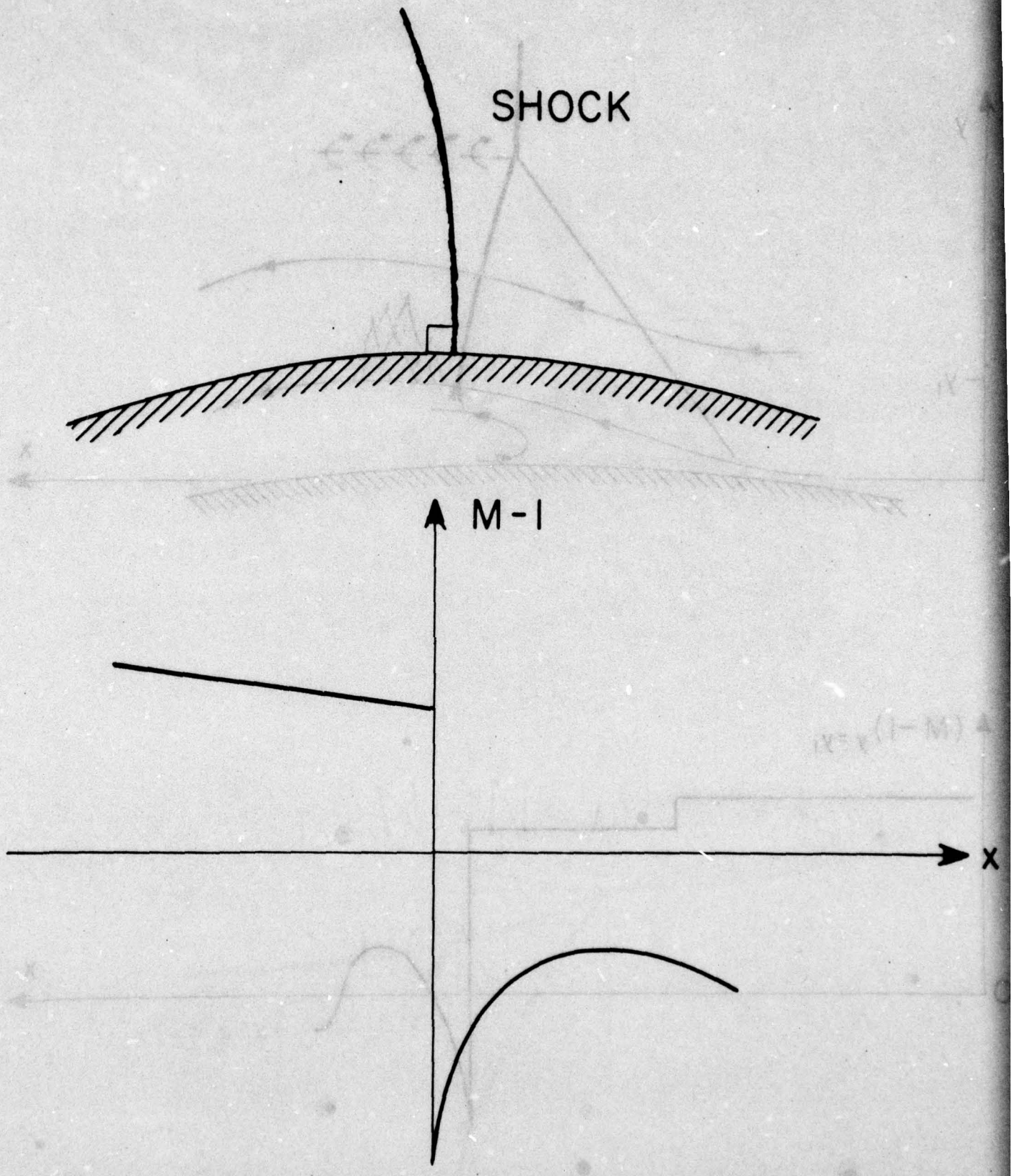

Fig. 5 External Inviscid Flow on Curved Wall Neglecting Displacement Effect (Schematic)

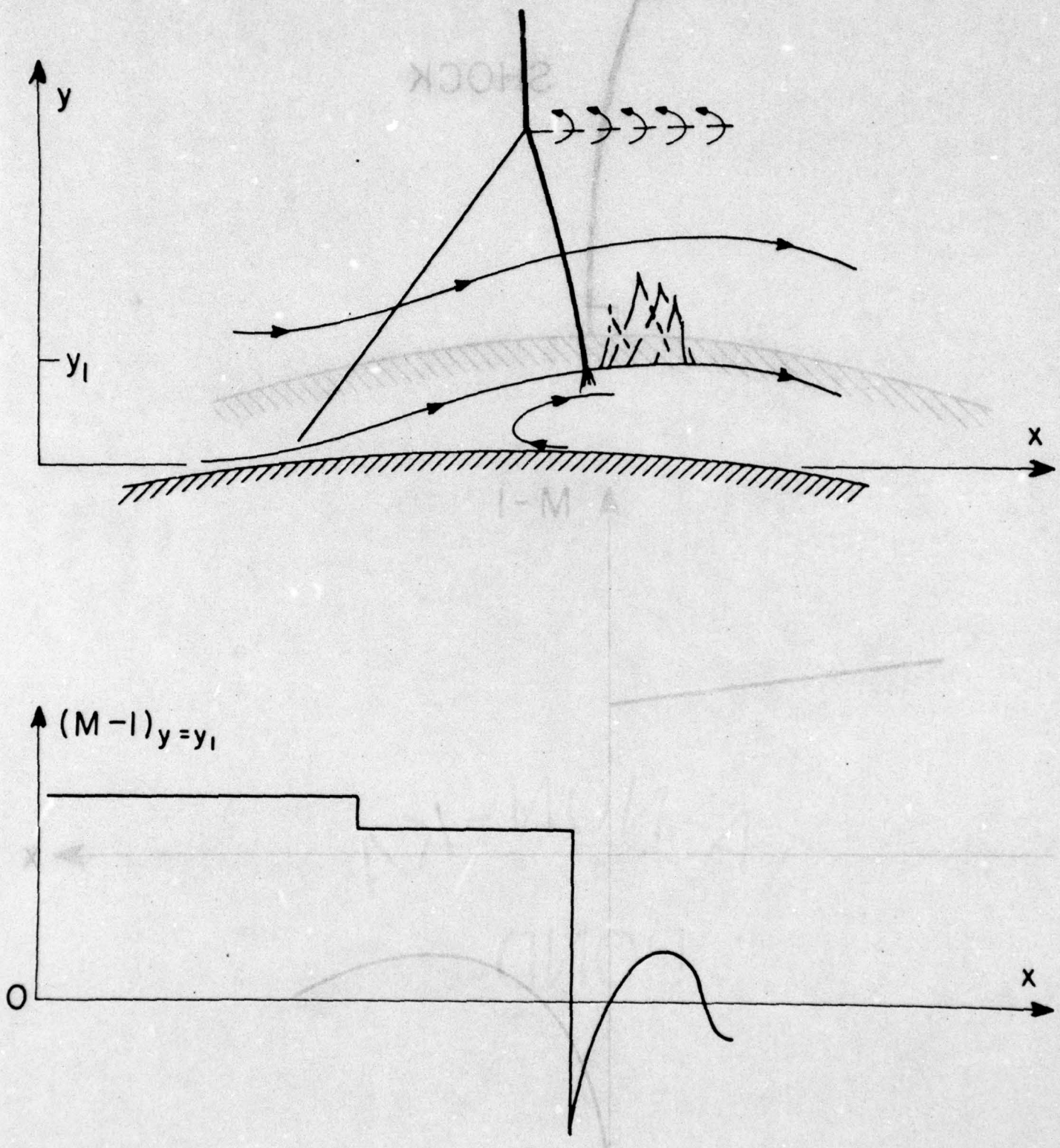

Fig. 6 Lambda-Shock Interaction Pattern for Separated Laminar Boundary Layers (after Ref. 4)

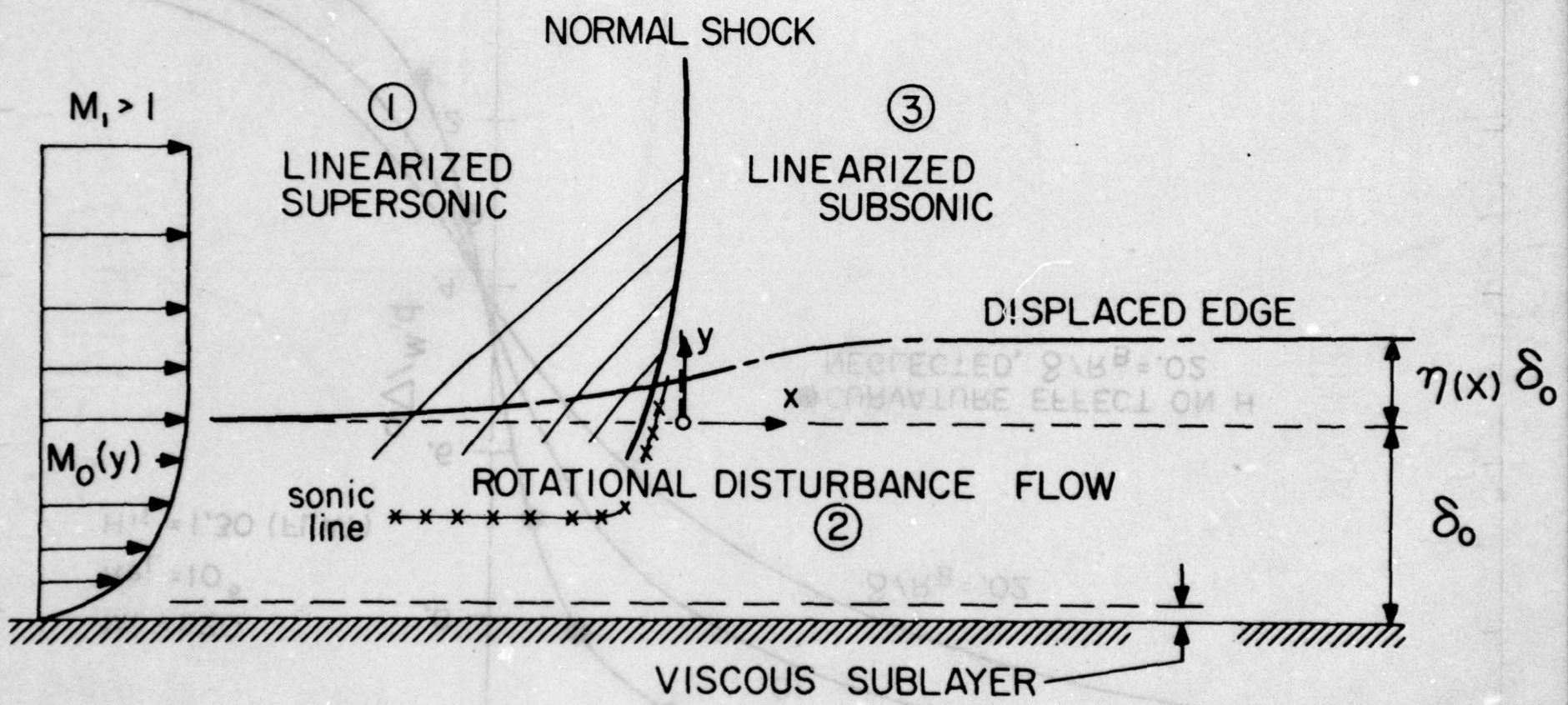

Fig. 7 Viscous-Inviscid Interaction Flow Model (Schematic)

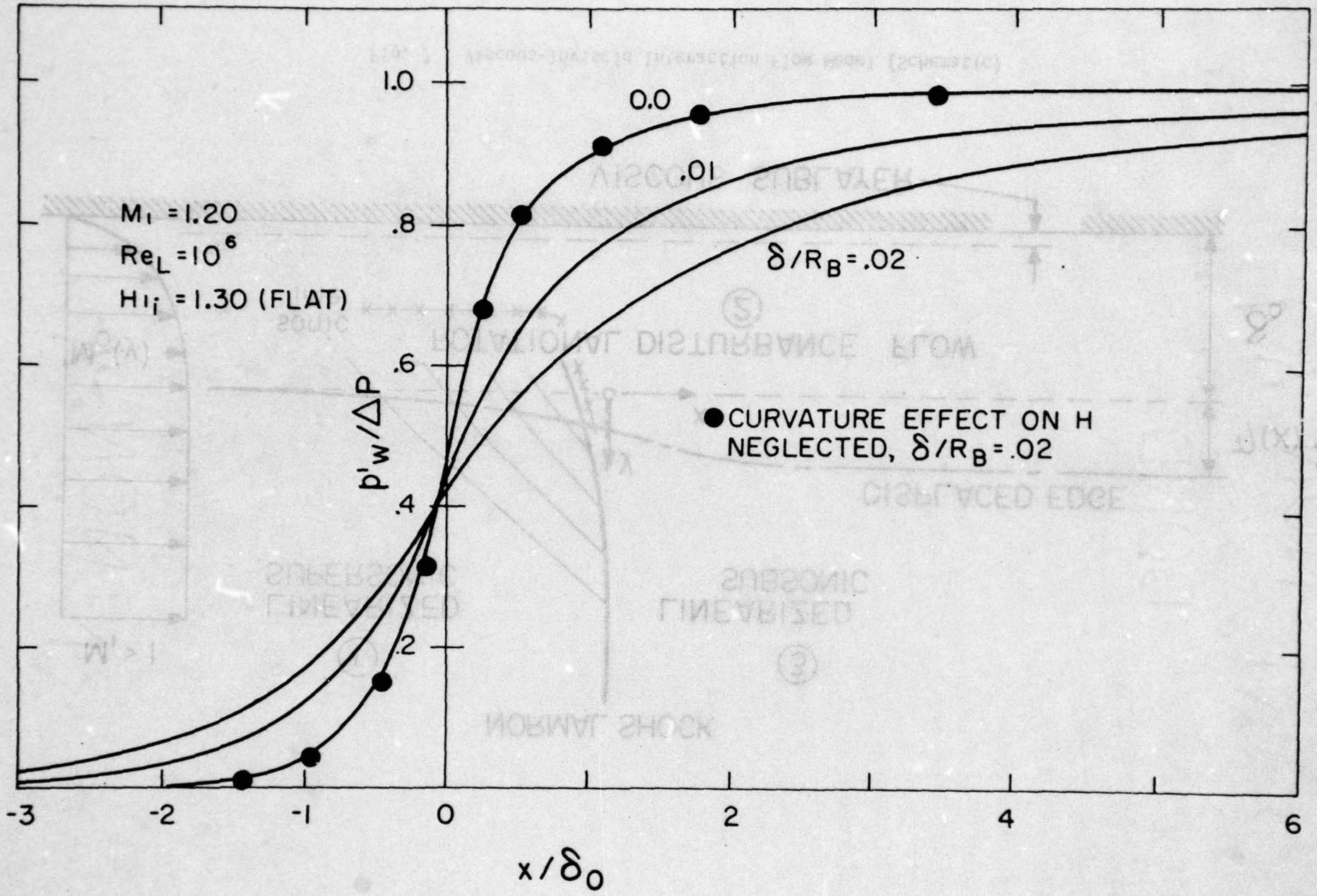

Fig. 8 Curvature Effect on Interaction Pressure Along the Wall

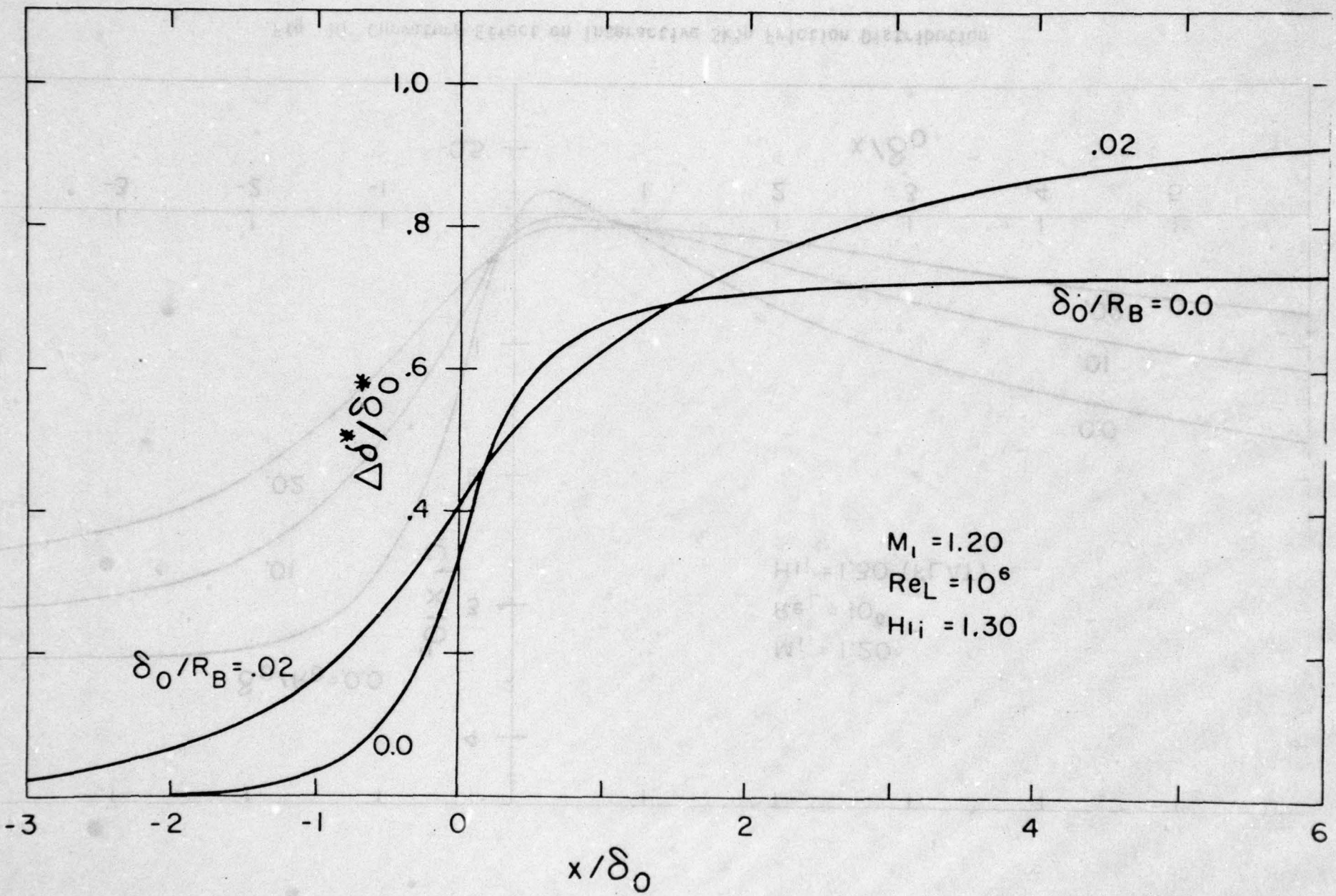

Fig. 9 Curvature Effect on Interactive Displacement Thickness Growth

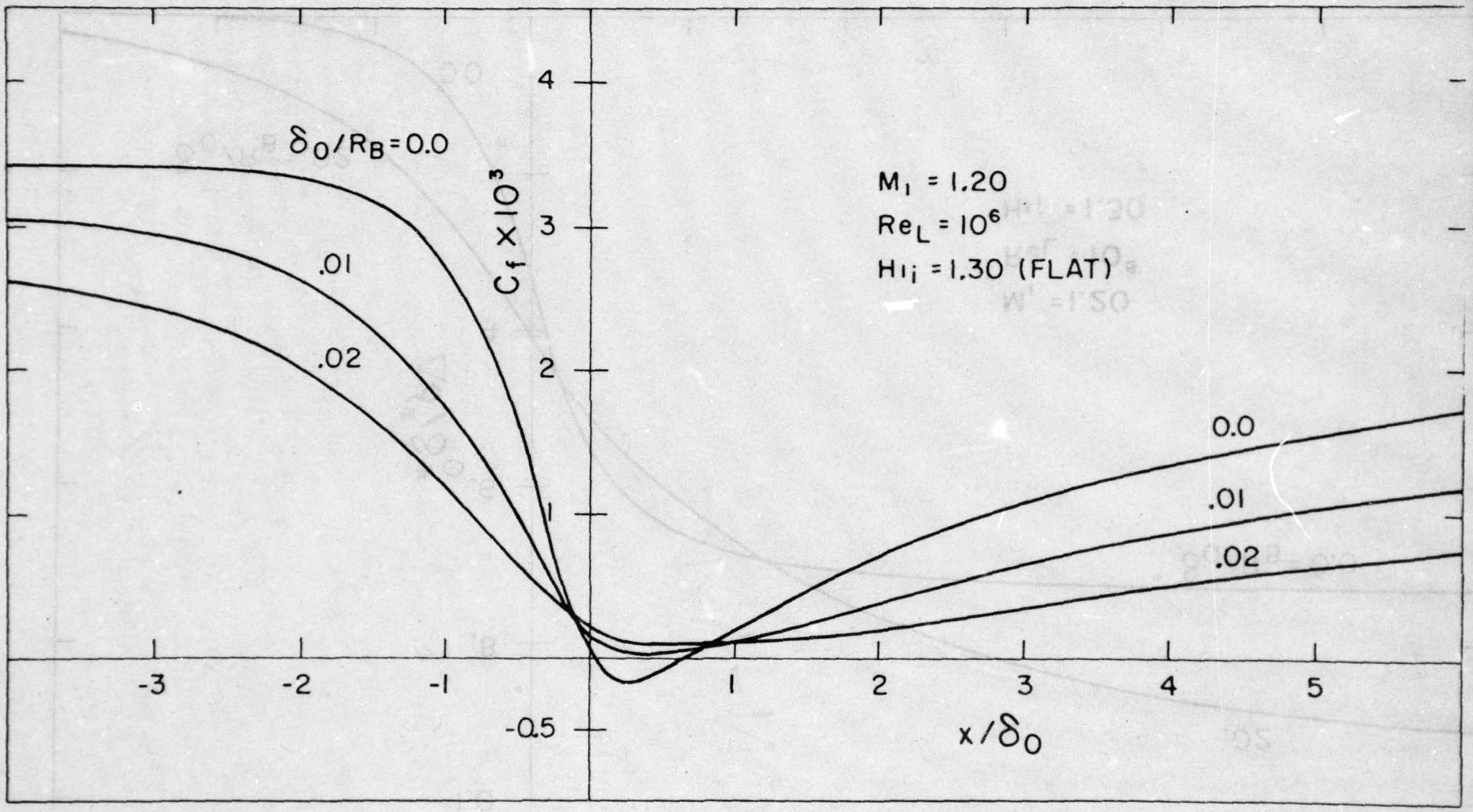

Fig. 10 Curvature Effect on Interactive Skin Friction Distribution

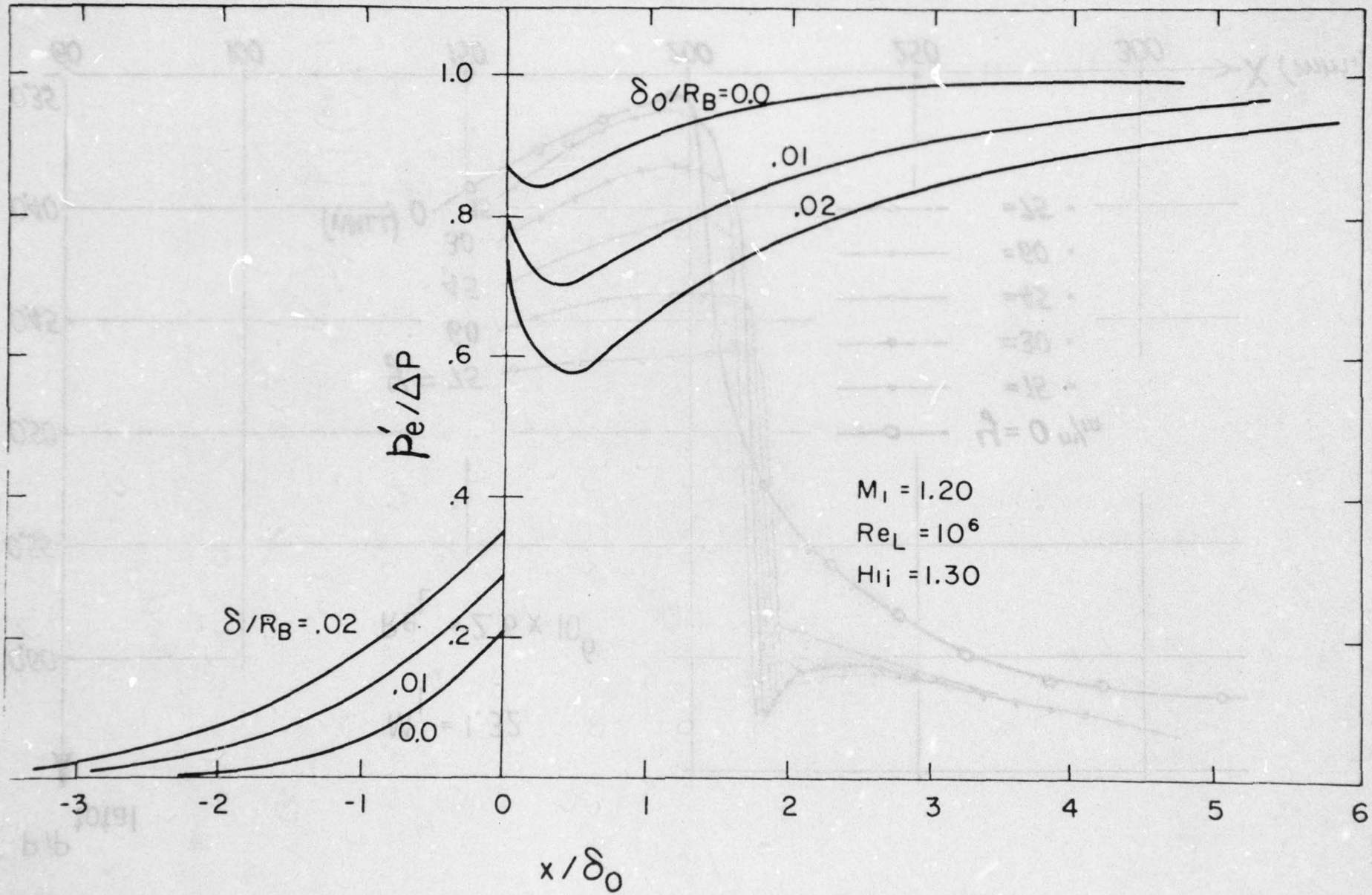

Fig. 11 Curvature Effect on Interaction Pressure Distribution Along Boundary Layer Edge

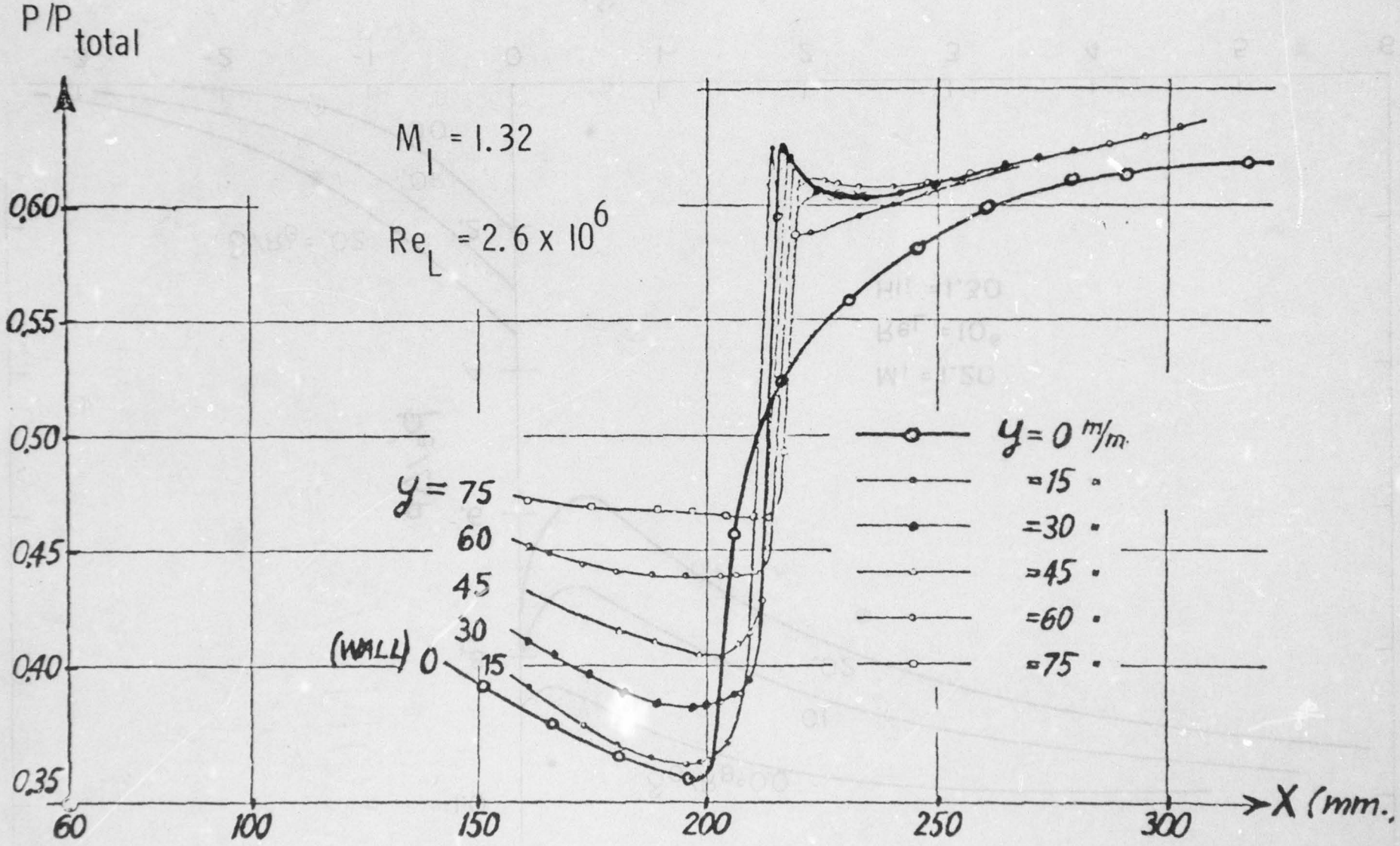

Fig. 12A Experimental Interaction Pressure Field (Ref. 4)

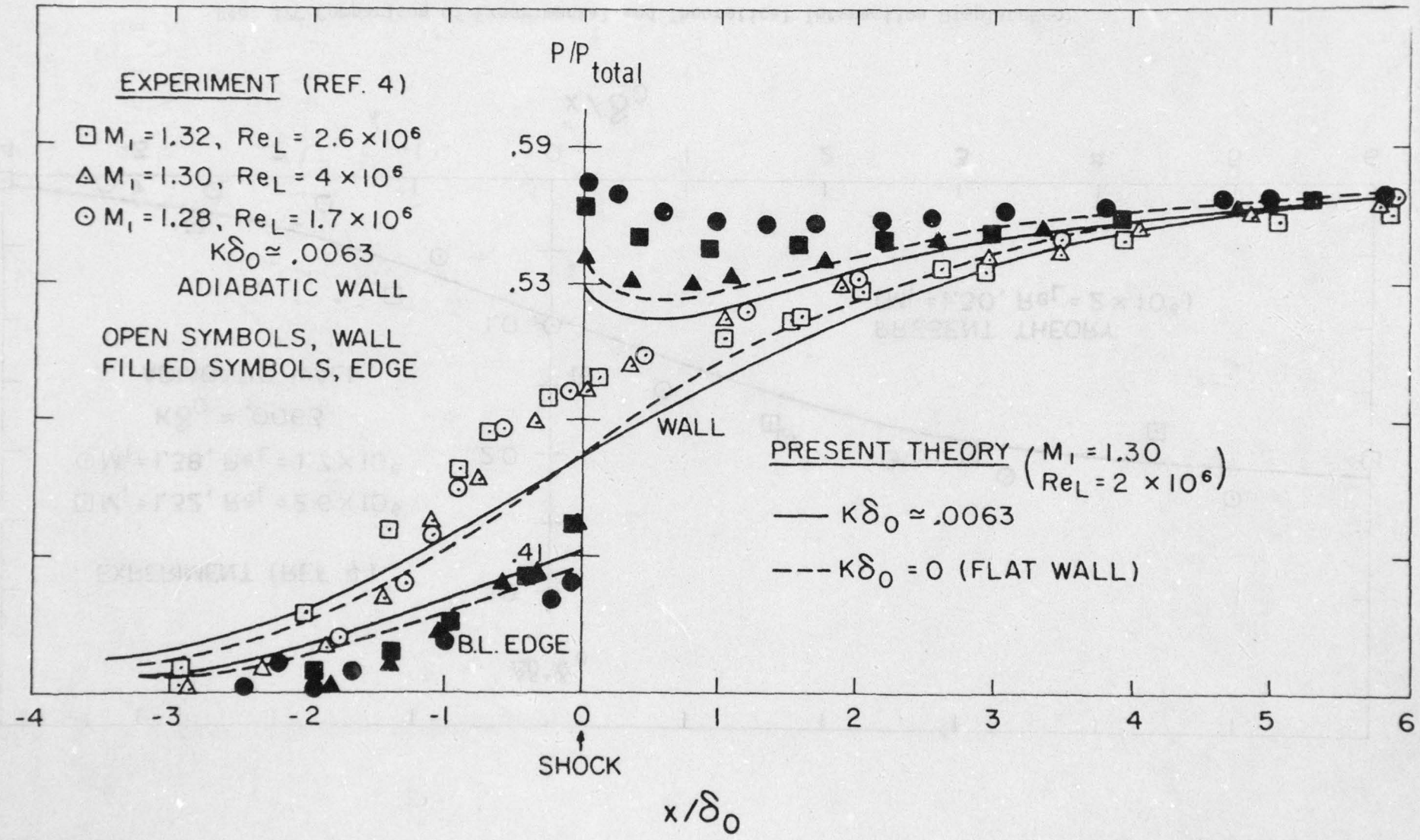

Fig. 12B Comparison of Present Theory with Experiment-Pressure Field

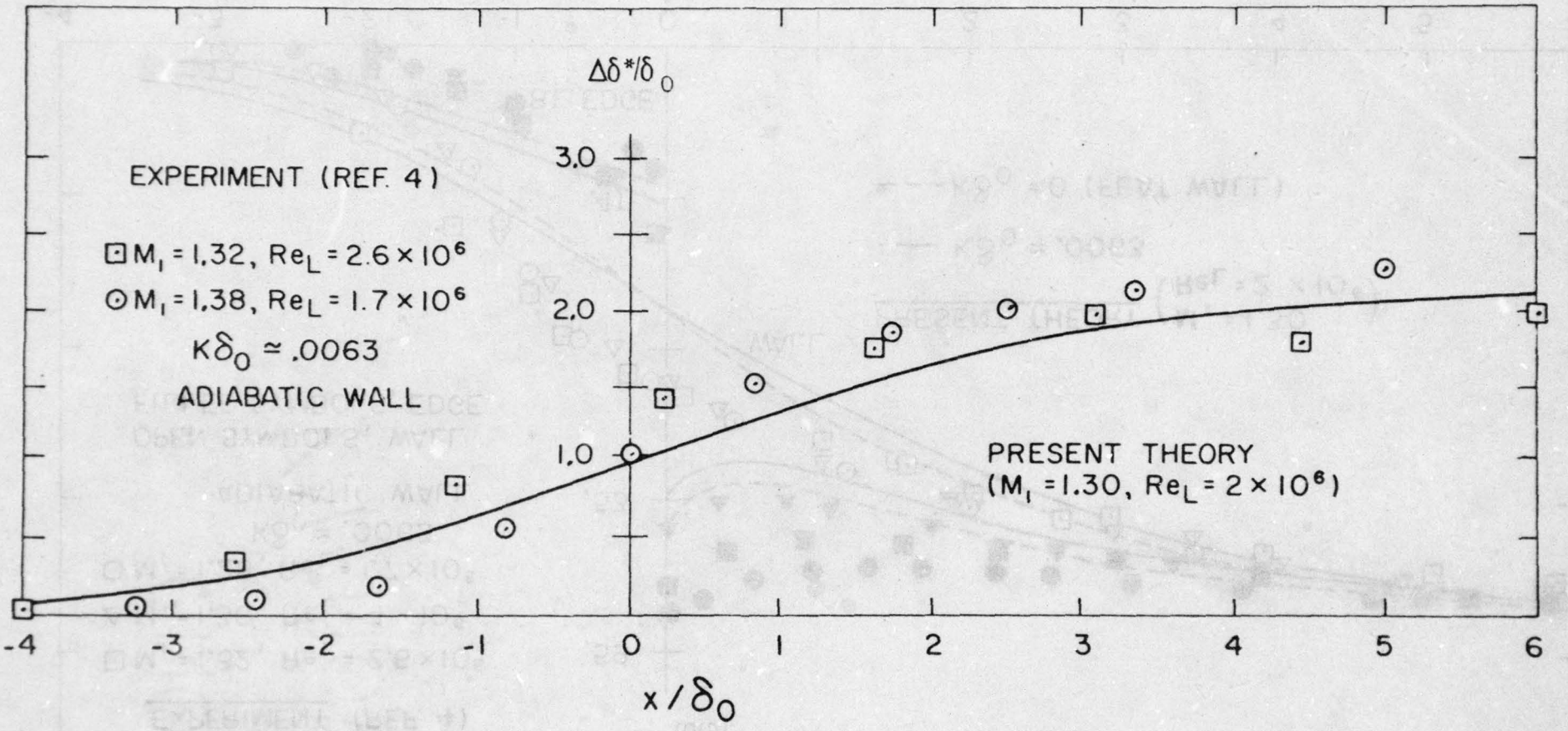

Fig. 12C Comparison of Experimental and Theoretical Interaction Displacement Thickness Distributions

SECURITY CLASSIFICATION OF THIS PAGE *(When Data Entered)*

REPORT DOCUMENTATION PAGE		READ INSTRUCTIONS BEFORE COMPLETING FORM
1. REPORT NUMBER VPI-AERO-088	2. GOVT ACCESSION NO.	3. RECIPIENT'S CATALOG NUMBER
4. TITLE *(and Subtitle)* NORMAL SHOCK INTERACTION WITH A TURBULENT BOUNDARY LAYER ON A CURVED WALL		5. TYPE OF REPORT & PERIOD COVERED 6. PERFORMING ORG. REPORT NUMBER
7. AUTHOR(s) G. R. Inger and H. Sobieczky		8. CONTRACT OR GRANT NUMBER(s) ONR N00014-75 C-0456
9. PERFORMING ORGANIZATION NAME AND ADDRESS Dept. of Aerospace and Ocean Engineering Virginia Tech. Blacksburg, Virginia 24061		10. PROGRAM ELEMENT, PROJECT, TASK AREA & WORK UNIT NUMBERS
11. CONTROLLING OFFICE NAME AND ADDRESS Office of Naval Research Fluid Dynamics Branch, Code 438 Arlington, Virginia Attn: Mr. Mort Cooper		12. REPORT DATE Oct. 1978 13. NUMBER OF PAGES 36
14. MONITORING AGENCY NAME & ADDRESS*(if different from Controlling Office)*		15. SECURITY CLASS. *(of this report)* Unclassified 15a. DECLASSIFICATION/DOWNGRADING SCHEDULE

16. DISTRIBUTION STATEMENT *(of this Report)*

Distribution unlimited

DISTRIBUTION STATEMENT A
Approved for public release; Distribution Unlimited

17. DISTRIBUTION STATEMENT *(of the abstract entered in Block 20, if different from Report)*

18. SUPPLEMENTARY NOTES

19. KEY WORDS *(Continue on reverse side if necessary and identify by block number)*

Transonic Shocks
Viscous-Inviscid Interaction
Longitudinal Curvature Effects

20. ABSTRACT *(Continue on reverse side if necessary and identify by block number)*

A detailed analysis is made of longitudinal surface curvature effects on the interaction of a weak normal shock with a non-separating two-dimensional turbulent boundary layer. It is shown that the interactive viscous displacement effect on the local outer inviscid transonic flow completely eliminates the well-known singularity pertaining to purely inviscid flow on a curved wall, i.e., the interactive pressure field is regular behind the shock. A study of the inner interaction solution within the boundary layer, however, reveals that curvature can

DD FORM 1 JAN 73 1473 EDITION OF 1 NOV 65 IS OBSOLETE

SECURITY CLASSIFICATION OF THIS PAGE *(When Data Entered)*

influence the interaction but for a hitherto-overlooked reason: the effect on the turbulent eddy viscosity, which alters the boundary layer profile shape upon which the interaction depends. An approximate non-asymptotic solution is given which incorporates this effect and example numerical results are presented and verified by comparison with experimental data. Small amounts of curvature ($K\delta \simeq .01$-$.02$) are found to moderately spread out and thicken the interaction zone while also beneficially delaying the onset of any incipient separation that occurs under the shock foot.